Molecular Microbiology (2015) 97(1), 125–138 ■
doi:10.1111/mmi.13014
First published online 24 April 2015

The *WOR1* 5' untranslated region regulates white-opaque switching in *Candida albicans* by reducing translational efficiency

Zhiyun Guan and Haoping Liu*
Department of Biological Chemistry, University of California, Irvine, CA, USA.

Summary

The human fungal pathogen *Candida albicans* undergoes white-opaque phenotypic switching, which enhances its adaptation to host niches. Switching is controlled by a transcriptional regulatory network of interlocking feedback loops acting on the transcription of *WOR1*, the master regulator of white-opaque switching, but regulation of the network on the translational level is not yet explored. Here, we show that the long 5′ untranslated region of *WOR1* regulates the white-opaque phenotype. Deletion of the *WOR1* 5′ UTR promotes white-to-opaque switching and stabilizes the opaque state. The *WOR1* 5′ UTR reduces translational efficiency and the association of the transcript with polysomes. Reduced polysome association was observed for additional key regulators of cell fate and morphology with long 5′ UTR as well. Overall, we find a novel regulatory step of white-opaque switching at the translational level. This translational regulation is implicated for many key regulators of cell fate and morphology in *C. albicans*.

Introduction

The diploid yeast *Candida albicans* is a major fungal pathogen of humans. *C. albicans* exists as a commensal in healthy individuals but can cause localized infection of mucosal membranes as well as systemic infection in immunocompromised patients. The phenotypic plasticity of *C. albicans* contributes to its success as a commensal and pathogen. In addition to the yeast-hyphal transition, *C. albicans* also undergoes switching between two epigenetically heritable phenotypic states, white and opaque (Slutsky *et al.*, 1987). Switching is stochastic and reversible and occurs approximately every 10^4 generations (Rikkerink *et al.*, 1988). White-to-opaque switching can be induced by environmental conditions, such as genotoxic stresses, N-acetyl-glucosamine (GlcNAc) as a carbon source and high CO_2 concentration (Ramirez-Zavala *et al.*, 2008; Alby and Bennett, 2009; Huang *et al.*, 2010). Growth at 37°C converts opaque cells to white (Bergen *et al.*, 1990). White and opaque cells exhibit distinct gene expression profiles, with 1306 genes transcribed differentially between the two states (Tuch *et al.*, 2010). In addition, white and opaque cells adapt to host defenses differently, with white cells more capable of causing infections in the bloodstream, whereas opaque cells are more efficient in colonizing skin, and in escaping macrophage detection (Kvaal *et al.*, 1999; Lachke *et al.*, 2003; Lohse and Johnson, 2008). Opaque cells are mating-competent, and *MTLa* or *MTLα* opaque cells mate with 10^6 greater efficiency compared with white cells. In *MTLa/α* cells, the a1-α2 heterodimer represses opaque formation (Miller and Johnson, 2002). Although the majority of natural *C. albicans* isolates are *MTLa/α*, a recent study has shown that passage through the mammalian gut promotes a phenotypic switch of *MTLa/α* cells to opaque-like cells that are more fit for GI colonization and commensalism (Pande *et al.*, 2013). In addition, *MTLa/α* cells are capable of opaque formation under high CO_2 and with GlcNAc as a carbon source, conditions that mimic the host environment (Xie *et al.*, 2013). These findings support the notion that white-opaque switching can occur in a majority of *C. albicans* strains and is highly relevant to *Candida*–host interactions.

The master regulator of white-opaque switching is *WOR1*, which is highly expressed in opaque cells and required for switching to opaque (Huang *et al.*, 2006; Srikantha *et al.*, 2006; Zordan *et al.*, 2006). Wor1 protein contains a novel DNA-binding domain (Lohse *et al.*, 2010; 2014; Zhang *et al.*, 2014) and promotes its own expression by binding to the *WOR1* promoter up to 8 kb upstream of its transcription start site (Zordan *et al.*, 2007). White-opaque switching and *WOR1* transcription are regulated by a circuit of interlocking transcriptional feedback loops, consisting of regulators *WOR1*, *EFG1*, *CZF1*, *WOR2*, *WOR3* and *AHR1* (Downs *et al.*, 2004; Levchenko and Jackson, 2004; Zordan *et al.*, 2007; Hernday *et al.*, 2013; Lohse

Accepted 30 March, 2015. *For correspondence. E-mail h4liu@uci.edu; Tel. (+1) (949) 824 1137; Fax (+1) (949) 824 2688.

et al., 2013). Notably, most of the regulatory genes in this circuit have a long 5′ untranslated region (5′ UTR): for example, the *WOR1* 5′ UTR is 1997 bp, *EFG1* 1139 bp, *CZF1* 1662 bp (Srikantha *et al*., 2006; Bruno *et al*., 2010; Tuch *et al*., 2010). In contrast, 5′ UTRs of other *C. albicans* genes that are not in the regulatory circuits for cell fate or yeast-hyphal regulation are mostly under 100 bp in length. Most yeasts, such as *Saccharomyces cerevisiae*, do not have genes with long 5′ UTRs (Nagalakshmi *et al*., 2008; Bruno *et al*., 2010). Although the transcriptional regulation of *WOR1* and white-opaque switching has been extensively studied, functions of and regulation by long 5′ UTRs remain to be explored.

Although long 5′ UTRs are rare in yeasts, they are common in higher eukaryotes and in viral genes and are frequently linked to translational regulation, in particular translational repression (Pickering and Willis, 2005). A common mechanism for translational repression at the 5′ UTR is through RNA-binding proteins. For example, a developmentally regulated translational control at 5′ UTR by a meiosis-specific RNA-binding protein is critical for establishing the meiotic chromosome segregation pattern in *S. cerevisiae* (Berchowitz *et al*., 2013). Additional elements that have been shown to control translational efficiency at 5′ UTRs include upstream open reading frames (uORFs) and internal ribosome entry sites (IRESs) (Morris and Geballe, 2000; Hellen and Sarnow, 2001). In *S. cerevisiae*, cap-independent translation at IRESs in the 5′ UTR of a small subset of genes is required for invasive growth (Gilbert *et al*., 2007). A recent study has shown that *C. albicans GCN4* is translationally regulated by a uORF (Sundaram and Grant, 2014b). The length and structure of the 5′ UTR also affect microRNA-mediated translational repression (Meijer *et al*., 2013). Finally, secondary structures in the 5′ UTR can inhibit translation by stalling translational initiation (Jackson *et al*., 1996; Jackson and Gorovsky, 2000). In *C. albicans*, translational inhibition by a long 5′ UTR has been observed for the hyphal-specific transcriptional regulator *UME6* (Childers *et al*., 2014). The long 5′ UTR of *WOR1* makes it a promising candidate as a cis-regulatory element of *WOR1* translation, and therefore of white-opaque switching.

In this study, we find that the *WOR1* 5′ UTR regulates the white-opaque phenotype by reducing translational efficiency of *WOR1*. We demonstrate that the 5′ UTR is repressive toward both opaque formation and stability. Deletion of the 5′ UTR greatly increases white-to-opaque switching while reducing opaque-to-white switching. We further show that translational repression at long 5′ UTRs is pervasive and is observed for several genes in *C. albicans*. As these genes are pivotal to yeast-hyphal and/or white-opaque transitions, we speculate that translational regulation at their 5′ UTR may also play an important role in cell fate commitment and maintenance.

Results

Deletion of the WOR1 *5′ UTR enhances white-opaque switching and opaque stability*

In order to examine the role of the *WOR1* 5′ UTR in white-opaque switching, we constructed strains in which the 5′ UTR was deleted, as shown in Fig. 1A and described in detail in *Experimental procedures*. In brief, the *WOR1p-Δ5′WOR1-HA* plasmid was constructed, in which the 5′ UTR sequence was removed by placing a 3 kb fragment of the *WOR1* promoter directly upstream of the *WOR1* coding sequence. A 5′ UTR-*WOR1*/Δ5′-*WOR1* strain was generated by integrating the *WOR1p-Δ5′WOR1-HA* at the *WOR1* promoter upstream of the *wor1Δ* locus of a *WOR1* heterozygous deletion mutant (5′ UTR-*WOR1/wor1*). Δ5′-*WOR1*/Δ5′-*WOR1* and Δ5′-*WOR1/wor1* strains were generated by transforming the *WOR1p-Δ5′WOR1-HA* into a *wor1Δ/wor1Δ* strain once and twice respectively (see *Experimental procedures*). In all three strains, the Δ5′ copy of *WOR1* was 3′-tagged with HA to facilitate additional assays. These Δ5′-*WOR1* strains were compared with 5′ UTR-*WOR1* strains for white-opaque switching frequency and opaque phase stability. White cells were grown on synthetic complete dextrose (SCD) plates at room temperature to assay spontaneous switching to opaque. After 7 days, all strains carrying Δ5′-*WOR1* displayed increased white-to-opaque switching, compared with corresponding strains carrying the same copy number of 5′ UTR-*WOR1* (Fig. 1B). The switching rate of 5′ UTR-*WOR1*/Δ5′-*WOR1* approached 100%, in contrast to 2% for wild-type cells of 5′ UTR-*WOR1*/5′ UTR-*WOR1* strain. Switching of 5′ UTR-*WOR1*/Δ5′-*WOR1* occurred as multiple opaque sectors per white colony, with entire colonies becoming opaque by 7 days. Intriguingly, the Δ5′-*WOR1*/Δ5′-*WOR1* strain had a 35.7% white-opaque switching rate, still substantially elevated from wild type but lower than 5′ UTR-*WOR1*/Δ5′-*WOR1*. Notably, the highest switching rate appeared to be conferred by heterozygosity for the *WOR1* 5′ UTR, suggesting both a positive and negative role for the 5′ UTR in regulation of switching. For cells carrying only one copy of *WOR1*, the absence of the 5′ UTR still conferred a higher switching rate. Compared with 5′ UTR-*WOR1/wor1*, which had a switching rate of only 1%, Δ5′-*WOR1/wor1* was able to switch to opaque at 12%. However, this was much lower than the Δ5′-*WOR1*/Δ5′-*WOR1* strain carrying two copies of *WOR1* (Fig 1B). The high white-opaque switching frequency raised the question of whether opaque state itself is more stably maintained in Δ5′-*WOR1* strains. Stability was assayed by incubating opaque cells of control and Δ5′-*WOR1* strains on solid media at room temperature or 37°C. We find that the presence of Δ5′-*WOR1* enhances opaque stability and reduces opaque-to-white switching (Fig. 1C). 5′ UTR-*WOR1*/Δ5′-*WOR1* and Δ5′-*WOR1*/Δ5′-*WOR1* showed less spontaneous opaque-white switching at room

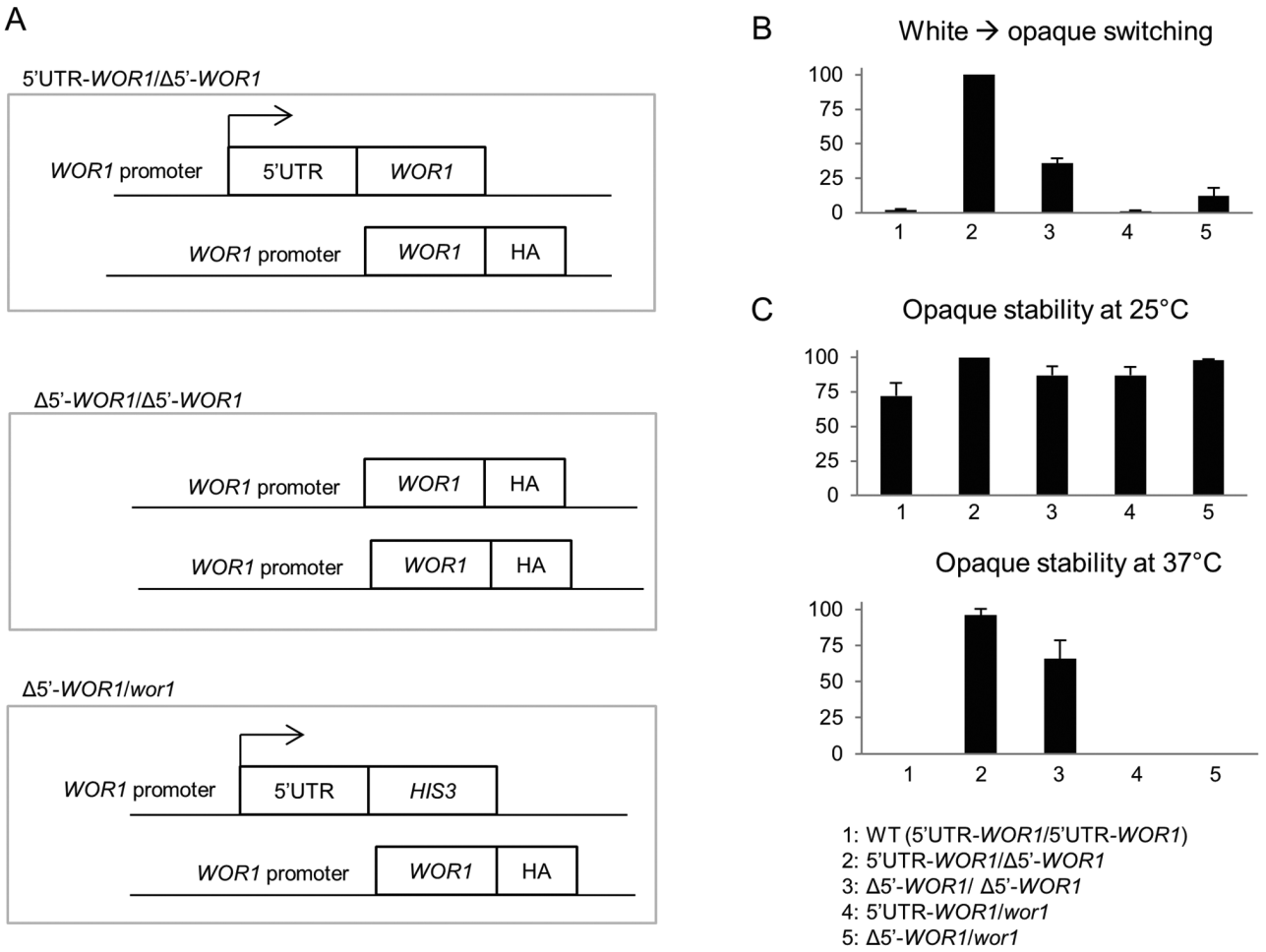

Fig. 1. Deletion of the 5′ UTR of *WOR1* promotes white-opaque switching and opaque stability.
A. Schematics of *WOR1* loci of the Δ5′-*WOR1* strains constructed for this study: 5′ UTR-*WOR1*/Δ5′-*WOR1*, Δ5′-*WOR1*/Δ5′-*WOR1* and Δ5′-*WOR1*/*wor1*.
B. Percentage of spontaneous white-opaque switching in the following strains; 1: 5′ UTR-*WOR1*/5′ UTR-*WOR1* (wild type; JYC1), 2: 5′ UTR-*WOR1*/Δ5′-*WOR1* (HLY4212), 3: Δ5′-*WOR1*/ Δ5′-*WOR1* (HLY4214), 4: 5′ UTR-*WOR1*/*wor1*(HLY3903) and 5: Δ5′-*WOR1*/*wor1* (HLY4213). White cells grown at 30°C were plated to SCD media and grown at room temperature (25°C) for 7 days before colony phenotype was scored.
C. Opaque stability of the strains described in (B). Opaque cells grown at 25°C were plated to SCD media and grown at 25°C and 37°C for 7 days. Stability of opaque state was measured as percentage of colonies that stay in opaque.

temperature than wild type, whereas Δ5′-*WOR1*/*wor1* also switched to white less frequently than 5′ UTR-*WOR1*/*wor1*. At 37°C, where opaque wild-type and 5′ UTR-*WOR1*/*wor1* cells switched *en masse* to white, nearly all 5′ UTR-*WOR1*/Δ5′-*WOR1* cells as well as 65.7% of Δ5′-*WOR1*/Δ5′-*WOR1* cells remained opaque after 7 days. However, all Δ5′-*WOR1*/*wor1* cells switched to white (Fig 1C). The highly opaque-switching and opaque-stable phenotype of cells carrying Δ5′-*WOR1* appears to be enhanced by increased copy number of *WOR1*, and in particular by having both 5′ UTR-*WOR1* and Δ5′-*WOR1*. As Δ5′-*WOR1* is HA-tagged, we needed to exclude the possibility that the HA tag produced this phenotype by affecting the stability/activity of Wor1. We compared the white-to-opaque switching rate of wild type strains with and without HA-tagged *WOR1* and found the presence of the HA tag on *WOR1* did not increase switching (Fig. S1, lanes 1 and 2). Having an additional untagged Δ5′-*WOR1* increased switching (lanes 2 and 3) to levels similar to HA tagged Δ5′-*WOR1* (lanes 3 and 4).

Deletion of the WOR1 *5′ UTR enhances* WOR1 *positive feedback at 37°C*

As *WOR1* transcription reflects the white-opaque phenotypic state of the cell, *WOR1* expression in strains carrying Δ5′-*WOR1* could illuminate the processes behind the higher opaque stability of Δ5′-*WOR1* strains. We examined

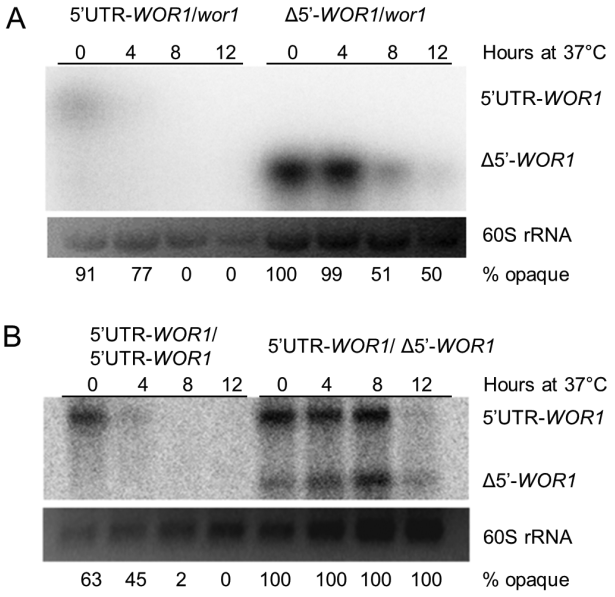

Fig. 2. Stabilization of *WOR1* expression at 37°C in Δ5′-*WOR1* strains.
Northern blot probing for a 500 bp region of the *WOR1* coding sequence against total RNA of A. initially opaque 5′ UTR-*WOR1/wor1* and Δ5′-*WOR1/wor1* cells, or B. initially opaque wild type (5′ UTR-*WOR1*/5′ UTR-*WOR1*) and 5′ UTR-*WOR1*/Δ5′-*WOR1* cells. Stably opaque cells were grown to log phase at 25°C, then transferred to 37°C. RNA was extracted every 4 h for Northern blotting, and white-opaque phenotype was assessed by removing cells to SCD plates, incubating at 25°C, then scoring colony phenotype after 4 days.

the effects of the 5′ UTR on *WOR1* transcript levels under conditions where wild-type opaque cells switch to white, but Δ5′-*WOR1* opaque cells remain mostly in opaque. To this end, we incubated at 37°C opaque cells of two strains that carry only one copy of *WOR1*: 5′ UTR-*WOR1/wor1* and Δ5′-*WOR1/wor1*. Northern blotting probing for *WOR1* was performed to compare transcript level in these two strains, sampled every 4 h (Fig. 2A). Cells from each time point were plated and grown on YPD plates at room temperature to determine percent of opaque cells. Prior to transfer to 37°C, *WOR1* transcript was more abundant in opaque Δ5′-*WOR1/wor1* cells than in 5′ UTR-*WOR1/wor1*. After cells were incubated at 37°C, *WOR1* transcript disappeared from the 5′ UTR-*WOR1/wor1* strain immediately but persisted for longer in the Δ5′-*WOR1/wor1* strain, with some transcript detectable 12 h after temperature shift (Fig. 2A). The opaque stability of cells removed from 37°C during the experiment was also higher for Δ5′-*WOR1/wor1* (Fig. 2A). The elevated level of Δ5′-*WOR1* transcript even at high temperature, assuming transcription levels are similar, presents the possibility of either heightened transcript stability or increased translation efficiency from the *Δ5′-WOR1*, which in turn promotes *WOR1* transcription through positive feedback of Wor1. To further examine the effect of the *Δ5′-WOR1* on *WOR1* positive feedback, we conducted Northern blotting under the same conditions on strains carrying two copies of *WOR1*: 5′ UTR-*WOR1*/5′ UTR-*WOR1* and 5′ UTR-*WOR1*/Δ5′-*WOR1* (Fig. 2B). At room temperature, 5′ UTR-*WOR1* transcript levels were similar in opaque cells of both strains. In the 5′ UTR-*WOR1*/Δ5′-*WOR1* strain, Δ5′-*WOR1* was present at a lower level than 5′ UTR-*WOR1*. This result suggested that the 5′ UTR of *WOR1* does not reduce its transcript level and in fact is correlated with more abundant transcript. Upon shifting to 37°C, *WOR1* transcript rapidly disappears in wild-type 5′ UTR-*WOR1*/5′ UTR-*WOR1* cells, whereas both 5′ UTR-*WOR1* and Δ5′-*WOR1* persist strongly for 8 or more hours in 5′ UTR-*WOR1*/Δ5′-*WOR1* and are still detectable at 12 h (Fig. 2B). Consistent with persistent *WOR1* transcription, a high percentage of cells remained opaque after treatment at 37°C compared with the wild-type control. We suggest that the stronger and more persistent expression of *WOR1* in the 5′ UTR-*WOR1/Δ5′-WOR1* strain is due to a stronger positive feedback from Wor1 protein, which is likely translated more efficiently from Δ5′-*WOR1* than from *5′UTR-WOR1*. The transcription from the Δ5′-*WOR1* construct likely initiated close to the promoter upstream of the annotated start codon, as the transcript from this construct was stable and efficiently translated into a functional Wor1 (Arribere and Gilbert, 2013). Transcriptional initiation at a downstream AUG will render the product non-functional as the next AUG is downstream of a significant portion of the DNA binding domain of Wor1.

5′ UTR-WOR1 *transcripts are enriched in monosome*

We suspected that 5′ UTR-*WOR1* is less efficiently translated than Δ5′-*WOR1*. Transcripts that are actively translated in the cell are associated with multiple ribosomes (polysomes), whereas those with stalled or less efficient translation are associated with ribosomal subunits or single 80S ribosomes (monosomes). Polysomes can be isolated by sedimentation of cell lysates (McQuillen *et al.*, 1959; Warner *et al.*, 1963). To determine the effect of the *WOR1* 5′ UTR on translational efficiency, we conducted a polysome gradient assay on the 5′ UTR-*WOR1*/Δ5′-*WOR1* strain, using opaque cells in which *WOR1* is expressed. Whole cell extract was separated by centrifugation on a sucrose gradient into fractions enriched for monosomes or polysomes, and absorbance profile was taken to visualize polysomal peaks (Fig. 3A). Ethylenediaminetetraacetic acid (EDTA) dissociated polysomes as expected (Fig. 3A). Monosomal and polysomal fractions were identified both based on absorbance profile and levels of 40S and 60S rRNA in each fraction as determined by reverse transcription quantitative PCR (RT-qPCR) on RNA extracted from each fraction (Fig. 3B). RT-qPCR was then used to deter-

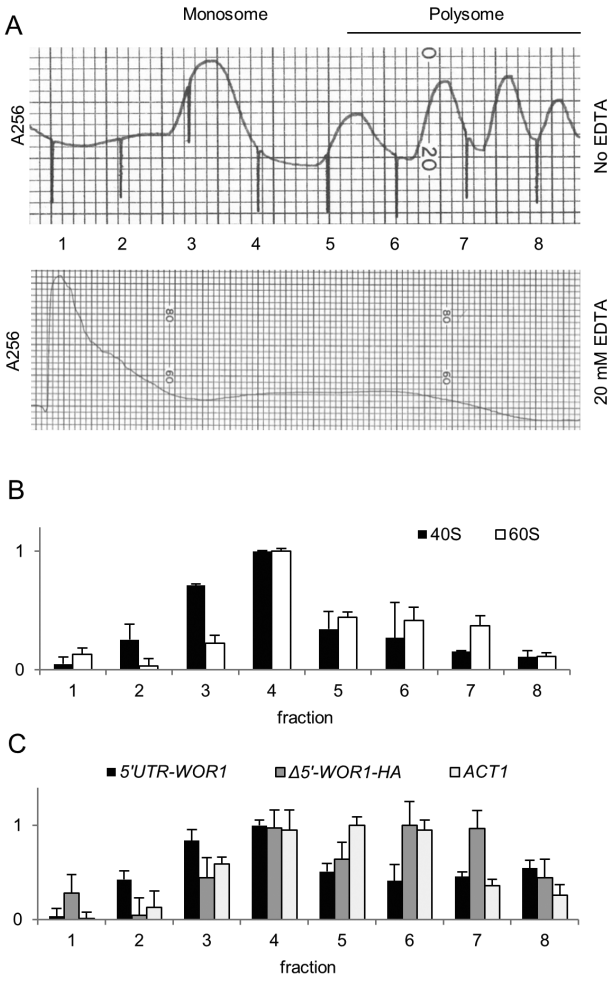

Fig. 3. 5′ UTR-*WOR1* transcripts are enriched in monosomes, whereas Δ5′-*WOR1* transcripts are enriched in polysomes.
A. Polysome profile of 5′ UTR-*WOR1*/Δ5′-*WOR1* opaque cells grown to log phase in YPD at room temperature (25°C). Cell lysate was applied to a sucrose gradient and centrifuged to separate monosomal and polysomal fractions. Fractions were collected in order of least to greatest density on an ISCO gradient fractionator, and absorbance profile taken at A254 nm. Absorbance profile of lysate applied to a gradient containing 20 mM EDTA is shown as negative control.
B. Relative abundance of 40S and 60S ribosomal RNA in each fraction.
C. Relative abundance of 5′ UTR-*WOR1*, Δ5′-*WOR1*-HA, and *ACT1* transcripts in each gradient fraction as determined by RT-qPCR. All experiments were performed in triplicate. For each transcript, values were normalized to the fraction containing the highest value, set as 1. Error bars represent standard deviation.

mine the level of monosomal and polysomal association of 5′ UTR-*WOR1* and Δ5′-*WOR1* transcripts. As Δ5′-*WOR1* is tagged at the 3′ end with -HA in this strain, primers amplifying a region extending from the 3′ end of the *WOR1* coding sequence to the -HA tag were used for detection of Δ5′-*WOR1* transcript. Primers amplifying a region of the *WOR1* 5′ UTR were used for detection of 5′ UTR-*WOR1* transcript. We found the distribution of 5′ UTR-*WOR1* to be highest in the monosome fractions and present at lower levels in the polysomal fractions. Conversely, Δ5′-*WOR1* transcript level showed higher association with polysomes, similar to *ACT1* (Fig. 3C). These results suggest less efficient translation of *WOR1* transcripts bearing the 5′ UTR, whereas Δ5′-*WOR1* transcripts are bound by multiple ribosomes and actively translated like *ACT1*.

The WOR1 *5′ UTR reduces translational efficiency*

Having established that transcripts containing the *WOR1* 5′ UTR are enriched in monosomes and less translated, we next sought to demonstrate that less Wor1 protein is made from the *5′ UTR-WOR1* transcript than from *WOR1* transcript without the 5′ UTR. To this end, the *WOR1* gene with or without its 5′ UTR was tagged with –HA and placed under the maltose-inducible *MAL2* promoter, resulting in the *MAL2p-5′UTR-WOR1-HA* or *MAL2p-WOR1-HA* plasmid. This allows for conditional expression without positive feedback of Wor1 onto its own promoter. Cells of WT + *MAL2p-5′UTR-WOR1-HA* or WT + *MAL2p-WOR1-HA* were transferred from dextrose to maltose to turn on expression from the *MAL2* promoter, upon which *WOR1* mRNA levels were assayed by RT-qPCR, and HA-tagged Wor1 protein by Western blotting (Fig. 4). At the transcript level, little difference was observed between 5′ UTR-*WOR1* or *WOR1*, indicating that the 5′ UTR did not function to reduce transcription. As the *MAL2* promoter is more active at higher temperature, transcript levels were elevated at 37°C, but again this was observed for both the 5′ UTR-*WOR1* and *WOR1* constructs (Fig. 4A). At the protein level, however, much higher levels of Wor1 were detected from *MAL2p-WOR1-HA* than *MAL2p-5′UTR-WOR1-HA*, pointing to significantly reduced translation when the 5′ UTR is present (Fig. 4B).

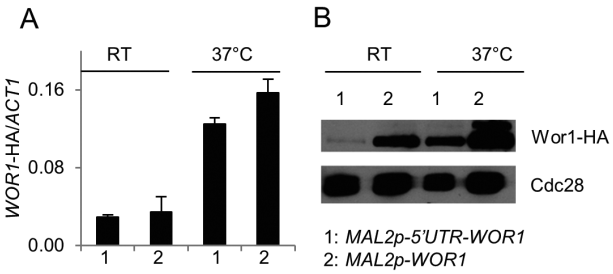

Fig. 4. *MAL2*-driven 5′ UTR-*WOR1* produces less Wor1 protein than *MAL2*-driven *WOR1*.
A. RT-qPCR of *WOR1* and B. Western blot detecting HA-tagged Wor1, in WT carrying *MAL2p-5′UTR-WOR1-HA* (HLY4215) or *MAL2p-WOR1-HA* (HLY3569). White cells were grown to log phase in YEP + dextrose, then inoculated to YEP + maltose to induce transcription from the *MAL2* promoter for 4 h at RT (25°C) or 37°C. For qPCR, all experiments were performed in triplicate, and values were normalized to *ACT1* signal.

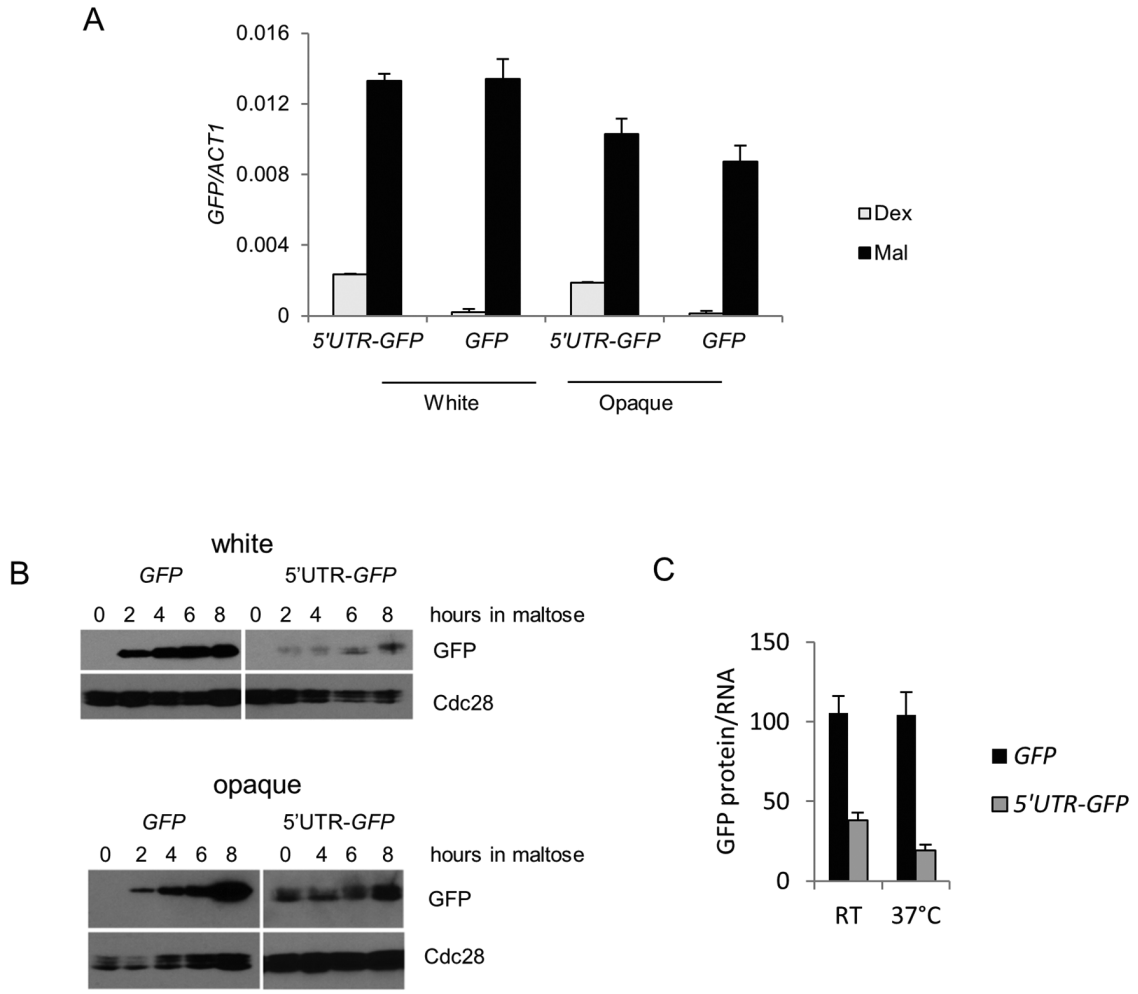

Fig. 5. The *WOR1* 5′ UTR represses translation of a downstream reporter at both room temperature and 37°C.
A. RT-qPCR of *GFP* mRNA and B. Western blot detecting GFP protein in white and opaque cells of WT + *MAL2p-WOR1 5′UTR-GFP* (HLY4216) and WT + *MAL2p-myc-GFP* (HLY4217).
C. Translational efficiency of GFP as a ratio of GFP fluorescence detected by FACS vs. GFP mRNA level as quantified by qPCR. Strains were grown to log phase in YEP + dextrose at RT, then inoculated to YEP + maltose at 37°C for 4 h to induce expression from the *MAL2* promoter. qPCR experiments were performed in triplicate and values were normalized to *ACT1*.

To determine whether the *WOR1* 5′ UTR was sufficient for the observed translational inhibition effect and the *WOR1* coding region did not contribute, we cloned (*WOR1*) 5′ UTR-*GFP* under the *MAL2* promoter to produce the *MAL2p-5′UTR-GFP* plasmid. A *MAL2p-myc-GFP* plasmid was used as a 5′ UTR-less control. White and opaque wild-type cells transformed with either plasmid were again transferred from dextrose to maltose to turn on expression from the *MAL2* promoter. Transcript levels of GFP with and without the *WOR1* 5′ UTR were similar in maltose, as shown by qPCR (Fig. 5A). The *MAL2* promoter is not entirely shut off in dextrose in the *MAL2p-5′UTR-GFP* strain; however, this appears to be unrelated to the *WOR1* 5′ UTR as it was also observed for both the *MAL2p-5′UTR-WOR1-HA* and *MAL2p-WOR1-HA* strains (Fig. S2). In white cells, Western blots probing for GFP showed that higher protein levels were reached more quickly upon induction with *MAL2p-myc-GFP* than with *MAL2p-5′UTR-GFP*, demonstrating that the *WOR1* 5′ UTR is sufficient for reducing translational efficiency. Notably, opaque cells of *MAL2p-5′UTR-GFP* expressed more GFP protein than their corresponding white cells upon maltose induction (Fig. 5B). Thus, the difference in translational efficiency imparted by the 5′ UTR is less stark in opaque cells, suggesting less regulation by the 5′ UTR in this state. Similar results were seen by observing GFP fluorescence using fluorescence-activated cell sorting (not shown).

Because of the increased opaque stability by the Δ5′-*WOR1* at 37°C, we investigated whether the *5′ UTR* regulation is temperature dependent. As growth at 37°C favors

white state, a temperature-sensitive translational regulation by the 5′ UTR could provide a mechanism disfavoring opaque formation at this temperature. We compared translational efficiency (protein/mRNA ratio) of GFP between *MAL2p-5′UTR-GFP* and *MAL2p-myc-GFP* strains while inducing the *MAL2* promoter at room temperature or 37°C. The *WOR1* 5′ UTR had a repressive effect on translation at both RT and 37°C, with the effect being moderately stronger at 37°C. In the absence of the *WOR1* 5′ UTR, translational efficiency of *MAL2p-myc-GFP* was not affected by temperature (Fig. 5C). We found similar results for opaque cells (not shown); however, the *MAL2* promoter is poorly induced in opaque state at RT, so a different system would be needed to confirm this finding. Our data suggest that the *WOR1* 5′ UTR is not the major point of regulation by temperature in opaque stability.

Argonaute, Ssd1 and uncapped 5′ UTR-WOR1 *transcripts are not involved in translational regulation at the* WOR1 *5′ UTR*

Several possibilities exist for the mechanism of translational regulation by the *WOR1* 5′ UTR. One such possibility is through micro-RNA-directed translational repression. It has been demonstrated that translational repression by miRNAs interacts with the 5′ UTR of genes through the initiation factor eIF4A2, which unwinds 5′ UTR structure to allow binding of the 60S ribosomal subunit (Meijer *et al.*, 2013). Although RNAi is absent from *S. cerevisiae*, many other budding yeasts, including *C. albicans*, have functional Argonaute and Dicer proteins as well as small non-coding RNAs, suggesting a possible RNAi system (Liu *et al.*, 1996; Drinnenberg *et al.*, 2009) To test the possibility of translational repression of RNA transcripts by Argonaute, we examined whether *WOR1* 5′ UTR-associated translational repression is present in the absence of Argonaute (*AGO1*). An *ago1* mutant was constructed and transformed with *MAL2p-5′UTR-GFP* or *MAL2p-myc-GFP*. We found that in an *ago1* mutant, levels of GFP protein from the *5′ UTR-GFP* were still greatly reduced compared with *myc-GFP* absent the *WOR1* 5′ UTR, similar to data observed in wild type (Fig. 6A). This result is corroborated by fluorescence-activated cell sorting (FACS) measuring GFP fluorescence (Fig. S3). In addition, *GFP* mRNA transcripts from *5′UTR-GFP* and *myc-GFP* are found at similar levels in the *ago1* mutant (Fig. 6B), indicating that the difference in protein levels is due to translational and not transcriptional regulation. Therefore, Argonaute is not necessary for translational repression by the *WOR1* 5′ UTR. This is consistent with our observeration of the lack of an effect by *AGO1* deletion on white-opaque switching (not shown).

To examine alternate mechanisms of translational regulation, we considered the role of RNA-binding proteins

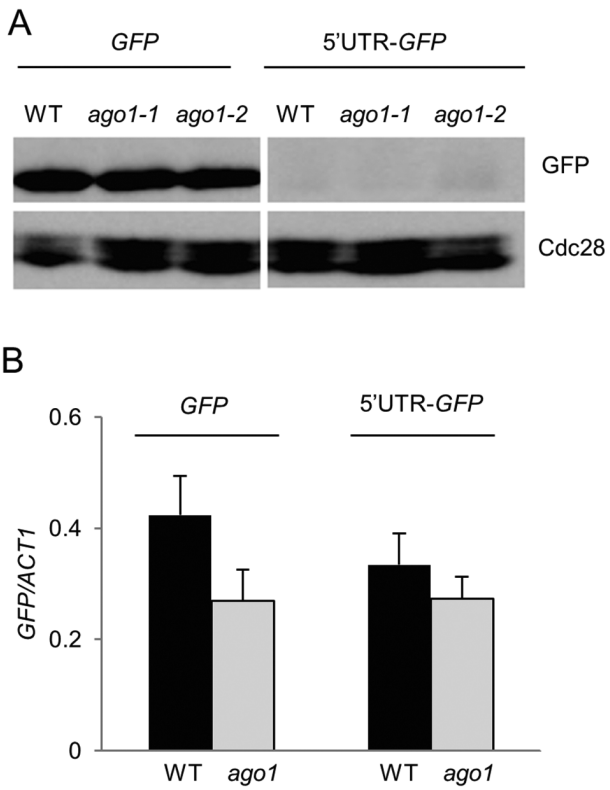

Fig. 6. Ago1 is not required for the translational repression by the *WOR1* 5′ UTR.
A. Western blot detecting GFP and B. *GFP*/*ACT1* transcript levels as detected by qRT-PCR from white cells of WT + *MAL2p-WOR1 5′UTR-GFP* (HLY4216), WT + *MAL2p-myc-GFP* (HLY4217), *ago1* (HLY3673) + *MAL2p-WOR1 5′UTR-GFP* (HLY4218) or *ago1* + *MAL2p-myc-GFP* (HLY4219). Two individual transformants from *ago1* mutant background were used (*ago1-1* and *ago1-2*). Strains were grown to log phase in YEP + dextrose, then inoculated to YEP + maltose for 4 h at 37°C to induce transcription from the *MAL2* promoter. GFP was detected with Clontech Living Colors anti-GFP antibody.

that may potentially interact with the *WOR1* 5′ UTR. In *S. cerevisiae*, Ssd1 is known to bind at the 5′ and 3′ UTR of specific mRNAs, reducing their translational efficiency (Cao *et al.*, 2006). Ssd1 activity is repressed by Cbk1, which is part of the RAM network critical for the regulation of cellular morphogenesis, polarized growth and septum destruction (Brooks and Jackson, 1994; Kolonko *et al.*, 2010; Lopes da Rosa *et al.*, 2010). Homologues of Cbk1, Ssd1 and downstream genes are present in *C. albicans*, where they are also critical for cell morphogenesis and mother–daughter separation (Jackson *et al.*, 1994; Lopes da Rosa *et al.*, 2013; Watanabe *et al.*, 2013). Considering that opaque cells are better separated than white cells between mother and daughters, the Cbk1-Ssd1 pathway could potentially be differentially regulated between white and opaque cells, and Ssd1 could be a candidate for translational repression at the *WOR1* 5′ UTR. If translational repression through the *WOR1* 5′ UTR is indeed

Table 1. Absence of uncapped 5′ UTR-*WOR1* transcripts as detected by qSL-RT-PCR.

		Ct transcript only	SD	Ct anchor-transcript	SD	Fold above background
ACT1	Ligase	14.08	0.04	32.15	0.15	9.13
	No ligase	15.08	0.10	36.34	0.21	
5'UTR-WOR1	Ligase	20.02	0.18	34.98	0.78	0.58
	No ligase	19.64	0.12	33.81	0.40	

Splint ligation was performed on RNA extracted from opaque wild-type cells, using DNA splints that facilitate the ligation of an RNA anchor oligo to uncapped *ACT1* or 5'UTR-*WOR1* RNA transcript. Reactions for which ligase was omitted were used as control for background. RNA was purified from ligation reactions and used for RT-PCR. Mean Ct values and standard deviation are shown for the amplification of each transcript as well as the ligated anchor-transcript region. Fold change above background was calculated as ΔCt. Experiments were performed in triplicate.

regulated through Ssd1, deletion of *SSD1* should reduce this repression. To investigate this, we transformed a *ssd1* deletion mutant (Zentner and Henikoff, 2013) with *MAL2p-myc-GFP* or *MAL2p-UTR-GFP*. FACS was performed to assess population-level GFP fluorescence as a reporter of translation in maltose-containing medium. We find that fluorescence of *MAL2p-5'UTR-GFP* is lower than that of *MAL2p-myc-GFP* in the *ssd1* mutant as in the wild-type control (Fig. S3). Thus, it appears that translational regulation through the *WOR1* 5′ UTR is not regulated by Ssd1.

Another possible mechanism of translational regulation by the *WOR1* 5′ UTR is cap-independent translation initiation. To explore this possibility, we sought to determine whether uncapped 5′ UTR-*WOR1* transcripts are normally found in the cell and at what levels. The splint-ligation-based qSL-RT-PCR method described by Blewett *et al*. was used to detect uncapped mRNA (Blewett *et al*., 2011). RNA was extracted from wild-type opaque cells, and ligation reactions performed to ligate the 5'UTR-*WOR1* RNA to an RNA anchor oligo, facilitated by a DNA splint homologous to both. Only RNA transcripts without the 5′ cap would be ligated to the anchor. RT-qPCR was then performed to detect both an amplicon within the original transcript (*WOR1* 5′ UTR) and one spanning the anchor and 5′ UTR. Detection of the second amplicon is indicative of successful ligation of an uncapped transcript. A ligase-free reaction was performed as a control. We find that with the addition of ligase, the detection of uncapped 5′ UTR-*WOR1* transcripts are 0.58-fold of ligase-free reaction, indicating that few, if any, 5′ UTR-*WOR1* transcripts exist in uncapped form. In comparison, detection of uncapped *ACT1* increases by 9.13-fold when ligase is added, demonstrating that the ligation reaction proceeds efficiently when uncapped transcripts exist (Table 1). Although the high level of uncapped *ACT1* transcript appears reflective of non-specific background decapping activity, this level of decapping is not seen for 5′ UTR-*WOR1* transcripts. These results indicate that the mechanism behind the lower translational efficiency of the *WOR1* 5′ UTR does not involve translation of uncapped transcripts. We also tested the possibility of alternative transcription originating within the *WOR1* 5′ UTR, resulting in shorter *WOR1* transcripts lacking all or part of the 5′ UTR. To assess whether these transcripts were produced and whether they appeared transiently during switching or in stable opaque cells, we used a strain carrying the *WOR1p*-5′UTR-*GFP and MAL2p-WOR1*. This would allow for induction of white-opaque switching by ectopically expressing *WOR1* under the *MAL2* promoter, whereas transcription from the *WOR1* promoter could be assayed through *GFP* RNA levels, without interference from ectopically expressed *WOR1*. Northern blotting was conducted to probe for *GFP*-containing RNA. As expected, the appearance of 5′ UTR-*GFP* RNA was correlated with switching to opaque. Although alternate transcription would have produced both a long (5′ UTR-*GFP*) and short (*GFP* only) transcript, we found *GFP* transcript of only one size, correlating to 5′ UTR-*GFP* at 2.7 kbp (Fig. S4). Thus, alternative transcription does not appear to initiate in the *WOR1* 5′ UTR.

Monosome association of 5′ UTR-containing transcripts extends to other key regulators of morphology in C. albicans

Although long 5′ UTRs are uncommon in *C. albicans*, they are notably present on a handful of genes regulating morphological switches (Bruno *et al*., 2010; Tuch *et al*., 2010). Key regulators of the yeast-hyphal transition, such as *RFG1* and *FLO8*, and of the white-opaque circuitry, such as *CZF1* and *EFG1* (also a hyphal regulator), all have 5′ UTRs in excess of several hundred to several thousand base pairs (Table 2). The length of the 5′ UTR in these genes raises the question of whether they possess a translational repressive activity like the *WOR1* 5′ UTR. To address this question, we conducted a polysome profile assay on wild-type opaque cells (Fig. 7A). The identification of monosome and polysome fractions was corroborated by 40S and 60S subunit content in each fraction as measured by RT-qPCR (Fig. 7B). Further RT-qPCR revealed that transcripts with long 5′ UTRs, such as *CZF1*, *EFG1*, *RFG1* and *FLO8*, were consistently enriched in

Table 2. 5′UTR length of key regulatory genes in *C. albicans*, based on transcriptome analysis by RNA-seq (Tuch *et al.*, 2010).

Gene name	5′ UTR length (bp)
CZF1	2071
WOR1	1978
RFG1	1267
EFG1	1139
FLO8	835
ACT1	72

monosomal fractions compared with polysomes, suggesting many of these transcripts are stalled in translational initiation or otherwise less efficiently translated. *ACT1*, which is actively translated and has a short 5′ UTR, displayed the opposite pattern and was more enriched in polysomes (Fig 7C). This result demonstrates that a long 5′ UTR is associated with reduced translational efficiency in key regulators of morphology in *C. albicans*.

Discussion

Extensive work has been done to characterize the network governing white-opaque switching in *C. albicans*, involving the master regulator *WOR1* and numerous other transcriptional regulators. However, much remains to be understood regarding the regulation of white-opaque switching at the translational level. In this study, we identify the *WOR1* 5′ UTR as a regulator of white-opaque switching that reduces the translational efficiency of *WOR1*. The *WOR1* 5′ UTR negatively regulates white-opaque switching and reduces the stability of the opaque cell state. We show evidence of reduced translational efficiency of 5′ UTR-*WOR1* both through polysome analysis, in which 5′ UTR-*WOR1* transcripts are more enriched in monosomes than polysomes, and through assays which demonstrate lower translation from 5′ UTR-*WOR1* than Δ5′-*WOR1* transcripts, even as transcription of the two remain the same. This effect is independent of the *WOR1* promoter and also of the *WOR1* coding region; placing the *WOR1* 5′ UTR upstream of another gene under an ectopic promoter produces the same reduction in translation. Therefore, the *WOR1* 5′ UTR is sufficient for the observed translational repression.

The mechanisms by which the *WOR1* 5′ UTR regulates translation leave ample room to be explored. There are numerous known mechanisms through which a 5′ UTR may affect translational efficiency. Within 5′ UTR regions themselves, uORFs and upstream AUG start codons (uAUGs) have been identified to regulate translation. Work in yeast has demonstrated that out-of-frame uAUGs can significantly alter the translational efficiency of a gene (Dvir *et al.*, 2013). In *C. albicans*, an example of translational regulation by a uORF has been demonstrated for the transcription factor *GCN4* (Sundaram and Grant, 2014b). The *WOR1* 5′ UTR contains no uORFS starting with AUG; however, uORFs with non-AUG start codons are another possibility, as ribosome profiling in *S. cerevisiae* has demonstrated pervasive translation initiating at non-AUG codons in 5′ UTRs (Ingolia *et al.*, 2009). Although potential non-AUG start codons such as GUG and UUG do exist in the *WOR1* 5′ UTR, ribosome profiling in *C. albicans* suggests that near-AUG codons have little effect on translation (Muzzey *et al.*, 2014). Therefore, it is unlikely that translational regulation by the *WOR1* 5′ UTR is mediated by uORFs. Secondary structures in the 5′ UTR are also known to negatively regulate translational efficiency, as stable structures can inhibit translational initiation. The secondary structure of the *WOR1* 5′ UTR and its effects on translation have yet to be determined due to the length of the 5′ UTR. Additional work has shown that the length and structure of 5′ UTRs impact

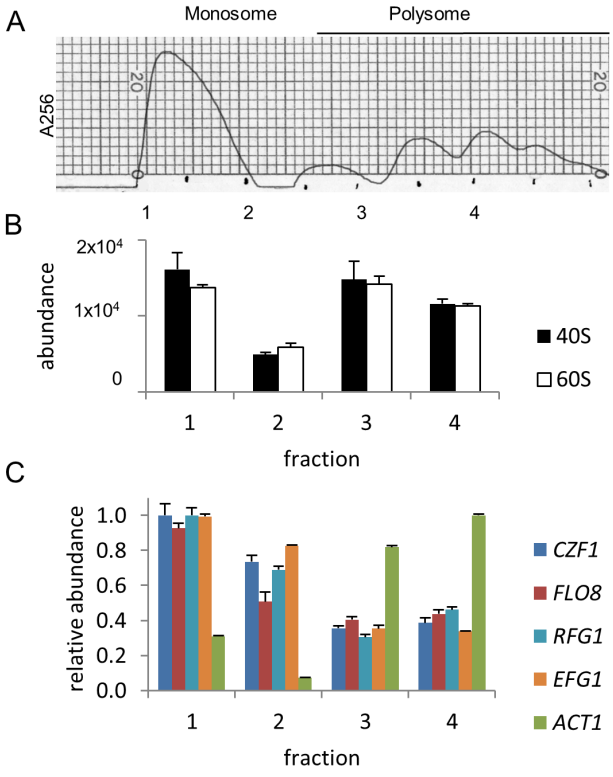

Fig. 7. Transcripts with long 5′ UTR are more enriched in monosome in *C. albicans*.
A. Polysome profile of wild-type (JYC5) opaque cells grown to log phase in YPD at room temperature.
B. 40S and 60S ribosomal subunit abundance in each fraction as determined by RT-qPCR.
C. Relative abundance in each fraction of transcripts of white-opaque regulatory genes *CZF1*, *FLO8*, *RFG1*, *EFG1*, as well as *ACT1*, as determined by RT-qPCR. Abundance of each transcript was normalized to the fraction containing the highest value.

translational repression by miRNAs through RNA interference (Meijer *et al*., 2013). *C. albicans* potentially has an intact RNAi system (Briggs *et al*., 1989). We tested the effect of Argonaute on 5′ UTR translational regulation and found that deletion of *AGO1* did not increase the translational efficiency of transcripts bearing the *WOR1* 5′ UTR. Thus, regulation through Argonaute appears an unlikely mechanism. It should be noted that Argonaute and Dicer appear insufficient for RNA interference in *C. albicans* (Liu *et al*., 1996), and other components of RNA silencing pathways may still affect *WOR1* transcript regulation.

Cap-independent translation initiating in the 5′ UTR provides an alternate mechanism for translational regulation. It is possible that cap-independent translation of 5′ UTR-*WOR1* occurs at a slower rate than cap-dependent translation and that this may be a dominant means of *WOR1* translation under some conditions. As a preliminary test, we assayed whether uncapped 5′ UTR-*WOR1* transcripts exist in opaque cells. We find that such transcripts are low, if not undetectable. Thus, the translation of uncapped RNAs does not appear to be a major mechanism regulating translation of 5′ UTR-*WOR1*.

Finally, RNA-binding protein activity at the 5′ UTR is another mechanism for translational regulation. One such example is Ssd1, which has been demonstrated to repress translation of specific genes by binding to their 5′ UTR and 3′ UTR in *S. cerevisiae* (Cao *et al*., 2006). Notably, Ssd1 represses translation of a specific subset of genes involved in cell morphogenesis and mother–daughter separation (Brooks and Jackson, 1994). Ssd1 targets genes expected to be highly expressed in opaque cells, making it a candidate for regulation at the *WOR1* 5′ UTR. We find that translational efficiency is reduced by the *WOR1* 5′ UTR in *ssd1* deletion mutant to a similar extent as wild type, so Ssd1 does not appear to regulate translation through the *WOR1* 5′ UTR. However, the role of numerous other RNA-binding proteins on the *WOR1* 5′ UTR remain to be tested. Whether the observed translational regulation at the 5′ UTR occurs through one of these proteins will require further exploration.

The identification of the *WOR1* 5′ UTR as a translational regulator of *WOR1* raises many questions for further investigation. The role of the 5′ UTR in translational regulation in higher eukaryotes has been extensively characterized, and in recent years studies in yeast have explored instances of UTR-mediated regulation as well. However, in *C. albicans*, the characterization of translational effect of 5′ UTRs has only begun. Recent work has shown that the *UME6* 5′ UTR, which is long and has predicted complex structure, reduces the translational efficiency of *UME6* and thereby negatively regulates filamentation (Childers *et al*., 2014). RNAseq studies in *C. albicans* have identified long 5′ UTRs on genes regulating white-opaque switching, hyphal morphogenesis and key processes in pathogenesis and commensalism. Our findings on *WOR1* identify a novel level of regulation for white-opaque switching through translation and support the possibility that key regulators of cell fate and cell morphology in *C. albicans* are translationally regulated through their 5′ UTRs. Further work may demonstrate roles for 5′ UTR on numerous other genes and characterize the mechanisms through which regulation occurs.

The ability of the *WOR1* 5′ UTR to regulate translational efficiency also raises questions on the biological impact of the 5′ UTR on white-opaque switching, as well as its role in helping *C. albicans* adapt to environmental changes. Of particular note is its relevance to the timescale of switching and the processes behind cell fate determination. White-opaque switching is slow, stochastic and infrequent. Even with ectopic expression of *WOR1*, many hours still pass before endogenous Wor1 protein is expressed at high levels, and switching is able to occur. The *WOR1* 5′ UTR provides one means through which opaque phase commitment is delayed. The reduced translational efficiency of *WOR1* conferred by the 5′ UTR may be a mechanism for preventing rapid switching to opaque during transient increases of *WOR1* transcription, such that commitment to opaque only occurs when long-term conditions are favorable to opaque state. Consistent with this notion, we find that the translational repression by the *WOR1* 5′ UTR is more pronounced in white than opaque cells. In addition, the *WOR1* 5′ UTR reduces stability of opaque state, which may allow opaque cells to switch back to white under conditions that no longer favor opaque. We have begun to test whether the *WOR1* 5′ UTR is a sensor of environmental conditions that affect white-opaque regulation. We found only a moderate change in 5′ UTR-mediated translational repression in response to 37°C, so the 5′ UTR is not a major thermosensor. In addition, we did not observe synergy between the switching phenotype of Δ5′-*WOR1* strains with CO2 and GlcNAc, which are known to induce white-opaque switching, making the 5'UTR less likely to be a sensor for these conditions. However, the role of the 5′ UTR in response to *in vivo* conditions that induce the expression of Wor1, such as those in the GI tract that promote formation of the opaque-like GUT phenotype (Pande *et al*., 2013), remain to be tested. Inhibition of translational initiation has recently been shown to be crucial to the response of *C. albicans* to oxidative stresses (Sundaram and Grant, 2014a). It will be of interest to explore further relationships between translational regulation and environmental signals in *C. albicans*. In this light, the 5′ UTR provides another layer of regulation that facilitates adaptation to long-term environmental changes without responding inappropriately to fluctuations in growth conditions. Regulation by the *WOR1* 5′ UTR promotes white phase stability and opaque-to-white switching, adding a layer of regulation to *WOR1*, which itself

promotes opaque. It will be intriguing to investigate whether 5′ UTR of other genes regulate cell fate through reducing or delaying switching and cell fate commitment.

Experimental procedures

Strains and culturing conditions

Strains used in this study are listed in Table S1. Strains were grown in YEP (1% yeast extract, 2% peptone) + 2% dextrose or maltose, or SCD (synthetic complete + 2% dextrose) media unless otherwise described. Colonies were maintained at room temperature (opaque cells) or 30°C (white cells).

Strain construction

Plasmid pMAL2-WOR1-HA was constructed in this lab as described by Huang *et al*. (Huang *et al*., 2006). Plasmid WOR1p-Δ5′WOR1-HA was modified from pMAL2-WOR1-HA by replacing the *MAL2* promoter with a fragment of the *WOR1* promoter 5081 to 1975 base pairs upstream of the start codon, excluding the 5′ UTR sequence. *WOR1p-Δ5′WOR1-HA* was digested with ClaI for integration at the ClaI site 4647 bp upstream of the *WOR1* start codon, and transformed into the strain *WOR1/wor1::HIS1* to produce 5′ UTR-*WOR1*/Δ5′-*WOR1*, or *wor1Δ* to produce Δ5′-*WOR1/wor1*. Transformants were selected for growth on SCD-ura. Integration of Δ5′-*WOR1* into the correct allele in the *WOR1/wor1::HIS1* background was verified by Southern blotting. To construct the Δ5′-*WOR1*/Δ5′-*WOR1* strain, the URA3 marker in Δ5′-*WOR1/wor1* was replaced with the SAT1 marker to confer nourseothiricin (NAT) resistance. The SAT1 marker driven by the *ACT1* promoter was amplified from plasmid pNIM1 (Ramirez-Zavala *et al*., 2008), with flanking sequences homologous to *URA3* introduced during amplification, then transformed into Δ5′-*WOR1/wor1*. NAT^R and *ura3*- strains were selected from colonies capable of growth on YPD + 200 mM NAT and incapable of growth on SCD-ura, then transformed again with plasmid WOR1p-Δ5′WOR1-HA, resulting in the Δ5′-*WOR1*/Δ5′-*WOR1* strain. Nourseothiricin was obtained as ClonNAT from WERNER BioAgents. The *MAL2p-5′UTR-WOR1-HA* plasmid was constructed by inserting a PCR amplification product containing the *WOR1* 5′ UTR into the XbaI site at the 5′ end of *WOR1* in pMAL2-WOR1-HA.

The *MAL2p-myc-GFP* plasmid was modified from the *MAL2p-myc-HGC* plasmid (Levchenko *et al*., 2005), by replacement of *HGC* with a 700 bp *GFP* fragment (Wunsch and Jackson, 2005). The *MAL2p-5′UTR-GFP* plasmid was modified from the *MAL2p-myc-GFP* plasmid by excision of the 13-myc tag via digestion with XbaI and MluI, and replacement with a PCR product containing the *WOR1* 5′UTR. All plasmids containing the *MAL2* promoter described in this study, unless otherwise specified, were digested with AscI for integration at the *ADE2* locus for transformation into *C. albicans*. The WT + *WOR1p-GFP* + *MAL2p-WOR1* strain was constructed as described (van Daal and Elgin, 1992).

The *ago1* mutant was constructed by deleting *AGO1* from the wild-type strain SN148 using the two-step PCR deletion method described by Noble and Johnson (Noble and Johnson, 2005). One copy of *AGO1* was replaced with *C. dubliniensis HIS1* from pSN52. Due to difficulty of directly replacing the second copy, a *MAL2p-AGO1-URA3* plasmid was transformed into the resulting *AGO1/ago1* strain and integrated at the *ADE2* locus. Subsequently, the remaining copy of *AGO1* at its native locus was replaced with *Candida maltosa LEU2* amplified from pSN40, and the *MAL2p-AGO1-URA3* insert eliminated by growth on 5-fluorootic acid (5'FOA). Complete deletion of *AGO1* was verified by PCR. The *MAL2p-AGO1-URA3* plasmid was modified from BES116 (Jackson, 1987). All primers used in strain construction are listed in Table S2.

Switching assays

Stable white or opaque cells from log-phase cultures were plated to SCD agar plates at a density of 100 cells $plate^{-1}$, using 100 μl of a dilution of 1000 cells ml^{-1}. Colony morphology was scored after 7 days. Both whole-colony and sectored switching events were counted. For white-opaque switching assays, plates were incubated at 25°C. For opaque stability assays, plates were incubated at 25 and 37°C.

Northern blotting

RNA was extracted from log-phase cultures using the Qiagen RNeasy kit. Northern blotting was conducted as described (Chen *et al*., 2002). A 500 bp PCR product of *WOR1* or *GFP* was used to probe for RNA containing the region of interest. Loading was assessed using a fragment of *ACT1* as probe, or with visualization of ribosomal RNA. Primers used for amplification of the *WOR1* probe are listed as WOR1probeF/R in (Huang *et al*., 2006).

Western blotting

Protein extraction was modified from (Meimoun *et al*., 2000). After precipitation with TCA as described, samples were washed once with acetone and boiled 5 min with equivolume urea buffer (8M urea, 4M 2-mercaptoethanol, 125 mM Tris pH 6.8 and 10% SDS), then centrifuged 5 min at 13 krpm. The supernatant was mixed with equivolume 20% glycerol + bromophenol blue and run on SDS-PAGE gels for Western blotting. The HA tag was detected with monoclonal rabbit anti-HA antibody from Abcam. GFP was detected with Living Colors monoclonal mouse anti-GFP antibody from Clontech. PSTAIRE (Cdc28) antibody was obtained from Invitrogen. Secondary IgG antibodies (anti-mouse or anti-rabbit) were obtained from Bio-Rad.

Polysome profiling

Polysome profiling was modified from (Masek *et al*., 2011). *C. albicans* cultures were grown to OD_{600} = 0.6, treated with 1 mg ml^{-1} cycloheximide, and incubated at 4°C for 5 min. Fifty milliliters of culture were collected for each sample. Extraction buffer was supplemented with 1 mg ml^{-1} cycloheximide. 7–47% sucrose gradients were prepared by stepwise freezing of 2.4 ml each of 7%, 17%, 27%, 37% and 47% sucrose in Beckman Coulter polyallomer centrifuge tubes at

–80°C, then thawing at 4°C overnight. For EDTA control samples, each gradient layer contained 20 mM EDTA. Lysate samples were applied to gradients and centrifuged at 35,000 r.p.m. at 4°C for 2.5 h in a Beckman SW41 rotor. Gradients were fractionated, absorbance was read at 254 nm, and polysome profile was created using the ISCO Gradient Fractionator (Teledyne). Fractions were collected using the Foxy Jr Fraction Collector. Fractions of 500 µl each were added to 800 µl 8 M guanidine HCl and 700 µl 100% EtOH, and placed at –20°C overnight for RNA precipitation. Pellets were washed with 70% EtOH and resuspended in 30 µl RNase-free water for subsequent use in RT-qPCR.

Quantitative PCR

cDNA was synthesized from 2 µg total RNA using the Bio-Rad iScript Reverse Transcription Kit. Quantitative PCR using the Bio-Rad SYBR Green mix was performed on the Bio-Rad iCycler. Cycle conditions were 95°C for 1 min, then 39 cycles of 95°C for 10 s, 56°C for 45 s, and 68°C for 20 s. Oligos used are listed in Table S2. All reactions were carried out in triplicate.

Splint ligation for qSL-RT-PCR

Ten micrograms of total RNA, 20 pmol of DNA splint and 30 pmol of RNA anchor were mixed and incubated at 70°C, 60°C, 42°C and 25°C, for 5 minutes at each step. The 20 U T4 DNA ligase (Invitrogen), T4 DNA ligase buffer and 20 U RNase Inhibitor Plus (Promega) were then added and ligation allowed to proceed overnight at 15°C. Ligase was omitted for control samples. Reactions were then treated with DNase using the Qiagen DNAse kit and protocols described therein. RNA was extracted using phenol/chloroform, precipitated with 1 ml 100% EtOH and 0.3M sodium acetate for 2 h at –20°C and washed once with 70% EtOH. RNA was then resuspended in 13.3 µl RNase-free water and used for RT-qPCR.

FACS

Fluorescence-activated cell sorting was conducted using the BD FACSCalibur system. FL1-H channel was used for GFP detection, and 10,000 cells were counted per sample. Results were analyzed with FlowJo cytometry analysis software.

Acknowledgements

We thank Shelley Lane for construction of the *ago1* strain and MAL2p-myc-GFP plasmid, and other members of the Liu lab for helpful discussion. We thank Dr. Jiangye Chen for the 5′ UTR-*WOR1/wor1* strain, Dr. Scott Filler for the *ssd1* strain, and Dr. Suzanne Noble for plasmids pSN40 and pSN52. We thank Dr. Suzanne Sandmeyer and Dr. Burt Semler for technical support with polysome gradient fractionation. Z.G. was supported by a National Library of Medicine Biomedical Informatics Training grant (5T15LM007443). This work was supported by the National Institutes of Health grants R01GM/AI55155 and R01AI099190 to H.L.

References

Alby, K., and Bennett, R.J. (2009) Stress-induced phenotypic switching in *Candida albicans*. *Mol Biol Cell* **20:** 3178–3191.

Arribere, J.A., and Gilbert, W.V. (2013) Roles for transcript leaders in translation and mRNA decay revealed by transcript leader sequencing. *Genome Res* **23:** 977–987.

Berchowitz, L.E., Gajadhar, A.S., van Werven, F.J., De Rosa, A.A., Samoylova, M.L., Brar, G.A., *et al.* (2013) A developmentally regulated translational control pathway establishes the meiotic chromosome segregation pattern. *Genes Dev* **27:** 2147–2163.

Bergen, M.S., Voss, E., and Soll, D.R. (1990) Switching at the cellular level in the white-opaque transition of *Candida albicans*. *J Gen Microbiol* **136:** 1925–1936.

Blewett, N., Coller, J., and Goldstrohm, A. (2011) A quantitative assay for measuring mRNA decapping by splinted ligation reverse transcription polymerase chain reaction: qSL-RT-PCR. *RNA* **17:** 535–543.

Briggs, D., Jackson, D., Whitelaw, E., and Proudfoot, N.J. (1989) Direct demonstration of termination signals for RNA polymerase II from the sea urchin H2A histone gene. *Nucleic Acids Res* **17:** 8061–8071.

Brooks, W., and Jackson, V. (1994) The rapid transfer and selective association of histones H2A and H2B onto negatively coiled DNA at physiological ionic strength. *J Biol Chem* **269:** 18155–18166.

Bruno, V.M., Wang, Z., Marjani, S.L., Euskirchen, G.M., Martin, J., Sherlock, G., and Snyder, M. (2010) Comprehensive annotation of the transcriptome of the human fungal pathogen *Candida albicans* using RNA-seq. *Genome Res* **20:** 1451–1458.

Cao, F., Lane, S., Raniga, P.P., Lu, Y., Zhou, Z., Ramon, K., *et al.* (2006) The Flo8 transcription factor is essential for hyphal development and virulence in *Candida albicans*. *Mol Biol Cell* **17:** 295–307.

Chen, J., Lane, S., and Liu, H. (2002) A conserved mitogen-activated protein kinase pathway is required for mating in *Candida albicans*. *Mol Microbiol* **46:** 1335–1344.

Childers, D.S., Mundodi, V., Banerjee, M., and Kadosh, D. (2014) A 5′ UTR-mediated translational efficiency mechanism inhibits the *Candida albicans* morphological transition. *Mol Microbiol* **92:** 570–585.

van Daal, A., and Elgin, S.C. (1992) A histone variant, H2AvD, is essential in *Drosophila melanogaster*. *Mol Biol Cell* **3:** 593–602.

Downs, J.A., Allard, S., Jobin-Robitaille, O., Javaheri, A., Auger, A., Bouchard, N., *et al.* (2004) Binding of chromatin-modifying activities to phosphorylated histone H2A at DNA damage sites. *Mol Cell* **16:** 979–990.

Drinnenberg, I.A., Weinberg, D.E., Xie, K.T., Mower, J.P., Wolfe, K.H., Fink, G.R., and Bartel, D.P. (2009) RNAi in budding yeast. *Science* **326:** 544–550.

Dvir, S., Velten, L., Sharon, E., Zeevi, D., Carey, L.B., Weinberger, A., and Segal, E. (2013) Deciphering the rules by which 5′-UTR sequences affect protein expression in yeast. *Proc Natl Acad Sci USA* **110:** E2792–E2801.

Gilbert, W.V., Zhou, K., Butler, T.K., and Doudna, J.A. (2007) Cap-independent translation is required for starvation-induced differentiation in yeast. *Science* **317:** 1224–1227.

Hellen, C.U., and Sarnow, P. (2001) Internal ribosome entry sites in eukaryotic mRNA molecules. *Genes Dev* **15:** 1593–1612.

Hernday, A.D., Lohse, M.B., Fordyce, P.M., Nobile, C.J., DeRisi, J.L., and Johnson, A.D. (2013) Structure of the transcriptional network controlling white-opaque switching in *Candida albicans*. *Mol Microbiol* **90:** 22–35.

Huang, G., Wang, H., Chou, S., Nie, X., Chen, J., and Liu, H. (2006) Bistable expression of WOR1, a master regulator of white-opaque switching in *Candida albicans*. *Proc Natl Acad Sci USA* **103:** 12813–12818.

Huang, G., Yi, S., Sahni, N., Daniels, K.J., Srikantha, T., and Soll, D.R. (2010) N-acetylglucosamine induces white to opaque switching, a mating prerequisite in Candida albicans. *PLoS Pathog* **6:** e1000806.

Ingolia, N.T., Ghaemmaghami, S., Newman, J.R., and Weissman, J.S. (2009) Genome-wide analysis in vivo of translation with nucleotide resolution using ribosome profiling. *Science* **324:** 218–223.

Jackson, J.D., and Gorovsky, M.A. (2000) Histone H2A.Z has a conserved function that is distinct from that of the major H2A sequence variants. *Nucleic Acids Res* **28:** 3811–3816.

Jackson, J.D., Falciano, V.T., and Gorovsky, M.A. (1996) A likely histone H2A.F/Z variant in Saccharomyces cerevisiae. *Trends Biochem Sci* **21:** 466–467.

Jackson, S., Brooks, W., and Jackson, V. (1994) Dynamics of the interactions of histones H2A,H2B and H3,H4 with torsionally stressed DNA. *Biochemistry* **33:** 5392–5403.

Jackson, V. (1987) Deposition of newly synthesized histones: new histones H2A and H2B do not deposit in the same nucleosome with new histones H3 and H4. *Biochemistry* **26:** 2315–2325.

Kolonko, E.M., Albaugh, B.N., Lindner, S.E., Chen, Y., Satyshur, K.A., Arnold, K.M., *et al*. (2010) Catalytic activation of histone acetyltransferase Rtt109 by a histone chaperone. *Proc Natl Acad Sci USA* **107:** 20275–20280.

Kvaal, C., Lachke, S.A., Srikantha, T., Daniels, K., McCoy, J., and Soll, D.R. (1999) Misexpression of the opaque-phase-specific gene PEP1 (SAP1) in the white phase of *Candida albicans* confers increased virulence in a mouse model of cutaneous infection. *Infect Immun* **67:** 6652–6662.

Lachke, S.A., Lockhart, S.R., Daniels, K.J., and Soll, D.R. (2003) Skin facilitates *Candida albicans* mating. *Infect Immun* **71:** 4970–4976.

Levchenko, V., and Jackson, V. (2004) Histone release during transcription: NAP1 forms a complex with H2A and H2B and facilitates a topologically dependent release of H3 and H4 from the nucleosome. *Biochemistry* **43:** 2359–2372.

Levchenko, V., Jackson, B., and Jackson, V. (2005) Histone release during transcription: displacement of the two H2A-H2B dimers in the nucleosome is dependent on different levels of transcription-induced positive stress. *Biochemistry* **44:** 5357–5372.

Liu, X., Li, B., and Gorovsky, M. (1996) Essential and nonessential histone H2A variants in *Tetrahymena thermophila*. *Mol Cell Biol* **16:** 4305–4311.

Lohse, M.B., and Johnson, A.D. (2008) Differential phagocytosis of white versus opaque *Candida albicans* by *Drosophila* and mouse phagocytes. *PLoS ONE* **3:** e1473.

Lohse, M.B., Zordan, R.E., Cain, C.W., and Johnson, A.D. (2010) Distinct class of DNA-binding domains is exemplified by a master regulator of phenotypic switching in *Candida albicans*. *Proc Natl Acad Sci USA* **107:** 14105–14110.

Lohse, M.B., Hernday, A.D., Fordyce, P.M., Noiman, L., Sorrells, T.R., Hanson-Smith, V., *et al*. (2013) Identification and characterization of a previously undescribed family of sequence-specific DNA-binding domains. *Proc Natl Acad Sci USA* **110:** 7660–7665.

Lohse, M.B., Rosenberg, O.S., Cox, J.S., Stroud, R.M., Finer-Moore, J.S., and Johnson, A.D. (2014) Structure of a new DNA-binding domain which regulates pathogenesis in a wide variety of fungi. *Proc Natl Acad Sci USA* **111:** 10404–10410.

Lopes da Rosa, J., Boyartchuk, V.L., Zhu, L.J., and Kaufman, P.D. (2010) Histone acetyltransferase Rtt109 is required for *Candida albicans* pathogenesis. *Proc Natl Acad Sci USA* **107:** 1594–1599.

Lopes da Rosa, J., Bajaj, V., Spoonamore, J., and Kaufman, P.D. (2013) A small molecule inhibitor of fungal histone acetyltransferase Rtt109. *Bioorg Med Chem Lett* **23:** 2853–2859.

McQuillen, K., Roberts, R.B., and Britten, R.J. (1959) Synthesis of nascent protein by ribosomes in *Escherichia coli*. *Proc Natl Acad Sci USA* **45:** 1437–1447.

Masek, T., Valasek, L., and Pospisek, M. (2011) Polysome analysis and RNA purification from sucrose gradients. *Methods Mol Biol* **703:** 293–309.

Meijer, H.A., Kong, Y.W., Lu, W.T., Wilczynska, A., Spriggs, R.V., Robinson, S.W., *et al*. (2013) Translational repression and eIF4A2 activity are critical for microRNA-mediated gene regulation. *Science* **340:** 82–85.

Meimoun, A., Holtzman, T., Weissman, Z., McBride, H.J., Stillman, D.J., Fink, G.R., and Kornitzer, D. (2000) Degradation of the transcription factor Gcn4 requires the kinase Pho85 and the SCF(CDC4) ubiquitin-ligase complex. *Mol Biol Cell* **11:** 915–927.

Miller, M.G., and Johnson, A.D. (2002) White-opaque switching in *Candida albicans* is controlled by mating-type locus homeodomain proteins and allows efficient mating. *Cell* **110:** 293–302.

Morris, D.R., and Geballe, A.P. (2000) Upstream open reading frames as regulators of mRNA translation. *Mol Cell Biol* **20:** 8635–8642.

Muzzey, D., Sherlock, G., and Weissman, J.S. (2014) Extensive and coordinated control of allele-specific expression by both transcription and translation in *Candida albicans*. *Genome Res* **24:** 963–973.

Nagalakshmi, U., Wang, Z., Waern, K., Shou, C., Raha, D., Gerstein, M., and Snyder, M. (2008) The transcriptional landscape of the yeast genome defined by RNA sequencing. *Science* **320:** 1344–1349.

Noble, S.M., and Johnson, A.D. (2005) Strains and strategies for large-scale gene deletion studies of the diploid human fungal pathogen *Candida albicans*. *Eukaryot Cell* **4:** 298–309.

Pande, K., Chen, C., and Noble, S.M. (2013) Passage through the mammalian gut triggers a phenotypic switch that promotes *Candida albicans* commensalism. *Nat Genet* **45:** 1088–1091.

Pickering, B.M., and Willis, A.E. (2005) The implications of structured 5′ untranslated regions on translation and disease. *Semin Cell Dev Biol* **16:** 39–47.

Ramirez-Zavala, B., Reuss, O., Park, Y.N., Ohlsen, K., and Morschhauser, J. (2008) Environmental induction of white-opaque switching in *Candida albicans*. *PLoS Pathog* **4:** e1000089.

Rikkerink, E.H., Magee, B.B., and Magee, P.T. (1988) Opaque-white phenotype transition: a programmed morphological transition in *Candida albicans*. *J Bacteriol* **170:** 895–899.

Slutsky, B., Staebell, M., Anderson, J., Risen, L., Pfaller, M., and Soll, D.R. (1987) 'White-opaque transition': a second high-frequency switching system in *Candida albicans*. *J Bacteriol* **169:** 189–197.

Srikantha, T., Borneman, A.R., Daniels, K.J., Pujol, C., Wu, W., Seringhaus, M.R., *et al*. (2006) TOS9 regulates white-opaque switching in *Candida albicans*. *Eukaryot Cell* **5:** 1674–1687.

Sundaram, A., and Grant, C.M. (2014a) Oxidant-specific regulation of protein synthesis in *Candida albicans*. *Fungal Genet Biol* **67:** 15–23.

Sundaram, A., and Grant, C.M. (2014b) A single inhibitory upstream open reading frame (uORF) is sufficient to regulate *Candida albicans* GCN4 translation in response to amino acid starvation conditions. *RNA* **20:** 559–567.

Tuch, B.B., Mitrovich, Q.M., Homann, O.R., Hernday, A.D., Monighetti, C.K., De La Vega, F.M., and Johnson, A.D. (2010) The transcriptomes of two heritable cell types illuminate the circuit governing their differentiation. *PLoS Genet* **6:** e1001070.

Warner, J.R., Knopf, P.M., and Rich, A. (1963) A multiple ribosomal structure in protein synthesis. *Proc Natl Acad Sci USA* **49:** 122–129.

Watanabe, S., Radman-Livaja, M., Rando, O.J., and Peterson, C.L. (2013) A histone acetylation switch regulates H2A.Z deposition by the SWR-C remodeling enzyme. *Science* **340:** 195–199.

Wunsch, A., and Jackson, V. (2005) Histone release during transcription: acetylation stabilizes the interaction of the H2A-H2B dimer with the H3-H4 tetramer in nucleosomes that are on highly positively coiled DNA. *Biochemistry* **44:** 16351–16364.

Xie, J., Tao, L., Nobile, C.J., Tong, Y., Guan, G., Sun, Y., *et al*. (2013) White-opaque switching in natural MTLa/alpha isolates of *Candida albicans*: evolutionary implications for roles in host adaptation, pathogenesis, and sex. *PLoS Biol* **11:** e1001525.

Zentner, G.E., and Henikoff, S. (2013) Regulation of nucleosome dynamics by histone modifications. *Nat Struct Mol Biol* **20:** 259–266.

Zhang, S., Zhang, T., Yan, M., Ding, J., and Chen, J. (2014) Crystal structure of the WOPR-DNA complex and implications for Wor1 function in white-opaque switching of *Candida albicans*. *Cell Res* **24:** 1108–1120.

Zordan, R.E., Galgoczy, D.J., and Johnson, A.D. (2006) Epigenetic properties of white-opaque switching in *Candida albicans* are based on a self-sustaining transcriptional feedback loop. *Proc Natl Acad Sci USA* **103:** 12807–12812.

Zordan, R.E., Miller, M.G., Galgoczy, D.J., Tuch, B.B., and Johnson, A.D. (2007) Interlocking transcriptional feedback loops control white-opaque switching in *Candida albicans*. *PLoS Biol* **5:** e256.

Supporting information

Additional supporting information may be found in the online version of this article at the publisher's web-site.